sciendo

Polish Journal of Chemical Technology, 24, 1, 1—6, 10.2478/pjct-2022-0002

An analytical model for wicking in porous media based on statistical geometry theory

Hui Gao[1], Guangyu Li[2,*], Zhongjing Wang[1], Nuo Xu[1], Zongyu Wu[3]

[1]*Beijing Institute of Mechanical Equipment, Beijing 100854, China*
[2]*School of Aircraft Engineering, Nanchang Hangkong University, Nanchang, Jiangxi 330063, China*
[3]*College of Aerospace Science and Engineering, National University of Defense Technology, Changsha, Hunan, 410073, China*
[*]*Corresponding author: e-mail: lgynudt@sina.com*

In this work, an analytical model describing liquid wicking phenomenon in porous media was constructed, based on the statistical geometry theory and the fractal theory. In the model, a new structure-property relationship, depicted by specific surface, porosity, tortuosity, pore fractal dimension, maximum pore size of the porous media, was introduced into the energy conservation equation. According to the theoretical model, the accumulated imbibition weight in porous media was achieved, and the predictions were verified by available experimental data published in different literatures. Besides, structure parameters influencing the imbibition process upon approaching equilibrium height were discussed. The model and results in this work are useful for the application of porous media in scientific research and industry.

Keywords: Wicking; Statistical geometry; Fractal; Porous media.

INTRODUCTION

The wicking behavior of liquid in porous media is a very important aspect of natural phenomena, its mechanism is widely used in scientific research and industry, for example, paper-based microfluidics[1], thermodynamic studies[2], oil recovery[3], advanced textile industry[4], and energy harvesting devices[5]. Since the introduction of the classical Lucas-Washburn equation[6], much more attention has been paid to its theoretical research and engineering applied science.

Wicking is the liquid being absorbed into the porous media by the action of the capillary pressure, generated by the difference in energies of dry and wet surfaces in the porous media. Numbers experiments have been carried out for measuring the wicking parameters of different porous media[7–11]. On the other hand, lots of researches have been done on studying the relation between the dynamics of the wicking rise and the porous media structure characteristics[12–16]. For the uncertainty and complexity of porous media, most research tries to describe the structure characters of porous media, and their influence on the wicking phenomenon. Trong Dang-Vu[17], Nate Stevens[18], and Kramer[19], studied the wicking rate in the sphere-like particles packed beds, set up models including diameter and surface area of the particles. Chan[20], Fries[21], and Tamayol[12], build the relationship between the wicking parameters, such as the permeability, and the porosity, tortuosity, of the porous media. However, most of these models are corrected by empirical parameters based on the experiment data, have a poor agreement with the natural porous media.

It was not easy to establish the theoretical relationship between the structure characters and the physical property of porous media until the development of the theoretical work on stochastic geometry[22]. Elsner[23] and Hermann[24] constructed the relationship between the effective dielectric and the geometry properties of porous media based on the new specific surface area and porosity models of the packed bed. Cai and Yu[16] described the pore nature and transport properties in porous media based on the fractal theory. Li and Zhao[25] established a mathematical model to predict the production rate by spontaneous imbibition, and this model predicts a power-law relationship between spontaneous imbibition rate and time.

The aim of the present work is to develop a general model for describing the wicking phenomenon in porous media, completely based on theoretical grounds. For this purpose, we established a new theoretical structure-property relationship based on the conclusions in stochastic geometry theory. And put it into the energy conservation equation of liquid rise in porous media, therefore, an analytical model was constructed. To verify the accuracy of this model, the accumulated imbibition weight in porous media was achieved, comparison was made between the predictions and available experimental data published in different literatures. At last, influences of the structure characters, such as specific surface, porosity and tortuosity, on approaching equilibrium height were discussed.

THEORY

Analytical model

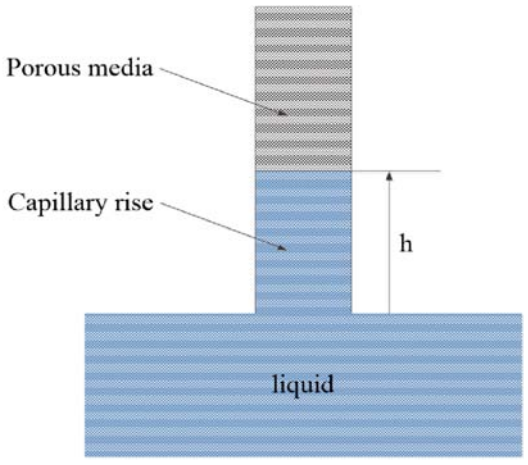

Figure 1. Sketch of capillary rise in porous media

During the liquid penetrating into the porous media, the system surface energy must be balanced by the viscous loss, the kinetic energy, and the gravitational potential energy the fluid obtained, according to the energy balance principle. As the dry solid-air interface area is reducing and the wetted solid-liquid interface area is increasing, the energy balance leads to[26]:

$$\gamma_s dA_{ls} - \gamma_w dA_{ls} = dE_v + dE_g + dE_k \tag{1}$$

Where, γ_s is the surface energy of the dry surface, γ_w stands for surface energy of the wetted surface areas, A_{ls} is the area of solid-liquid interface, E_v is viscous energy loss, E_g is the gravitational potential energy the fluid obtained and E_k is kinetic energy. According to Young's equation, the contact angle is introduced[27].

$$\cos\theta = \frac{\gamma_s - \gamma_w}{\gamma_l} \tag{2}$$

In equation (2), γ_l is the surface energy of the liquid. Figure 1 shows capillary rise in vertical porous media. In the porous media, the wetted surface is related to the height of capillary rise, h , the cross area A, and the specific surface S_v. Here, the specific surface S_v is an important structure parameter of the porous media, which is defined as the ratio of the surface area to the volume of the porous media, $S_v = S/V$, then

$$dA_{ls} = S_v A dh \tag{3}$$

Inserting equations (2) and (3) into equation (1), yields:

$$S_v A\gamma_l \cos\theta = \frac{dE_v}{dh} + \frac{dE_g}{dh} + \frac{dE_k}{dh} \tag{4}$$

For $dE = F \cdot dh$, the three terms in the right side of equation (4) can be vicious, gravity, and kinetic forces, respectively. Then,

$$S_v A\gamma_l \cos\theta = F_v + F_g + F_k \tag{5}$$

Darcy's law can be used to obtain the viscous pressure drop of liquid flow across the porous media. Its form may be simplified as

$$P_v = \frac{\mu h \dot{h}}{K} \tag{6}$$

Where P_v is the viscous pressure loss, μ is the dynamic viscosity, $\dot{h}$ is the average velocity of liquid inside the porous media, K is the permeability of the media. Here, it is assumed that porous media can be considered as a tortuous capillary. The tortuous path L_e may have an equal or longer distance, compared to the straight path L, then define the tortuosity τ as[16]:

$$\tau = \frac{L_e}{L} \tag{7}$$

And, Carman equation[28] the permeability is

$$K = \frac{\phi d_h^2}{32\tau^2} \tag{8}$$

Where, d_h is the hydraulic diameter, which is related to the structure of the porous media, ϕ is the porosity of the porous media, and both of them will be described in the next section. As the result, equation (6) can be written as follows:

$$P_v = 32\tau^2 \frac{h\mu\dot{h}}{\phi d_h^2} \tag{9}$$

Therefore, the viscous force associated with the above viscous pressure is:

$$F_V = 32\tau^2 \frac{h\mu\dot{h}}{\phi d_h^2} A \tag{10}$$

The gravitational force is the weight of the liquid sucked inside the porous media, and can be expressed as:

$$F_g = \rho g A \phi h \tag{11}$$

The kinetic force acts on the liquid, which depends on mass and velocity of the liquid. As both mass and velocity change with time, t, so:

$$F_k = \frac{d(m\dot{h})}{dt} = \rho A\phi \frac{d}{dt}(h\dot{h}) \tag{12}$$

Substituting expressions for viscous, gravitational, and kinetic force into equation (5), leads to the following expression for liquid-front movement in porous media:

$$S_v A\gamma_l \cos\theta = 32\tau^2 \frac{h\mu\dot{h}}{\phi d_h^2} A + \rho g A\phi h + \rho A\phi \frac{d}{dt}(h\dot{h}) \tag{13}$$

And:

$$S_v\gamma_l \cos\theta = 32\tau^2 \frac{h\mu\dot{h}}{\phi d_h^2} + \rho g\phi h + \rho\phi\left(h\ddot{h} + \dot{h}^2\right) \tag{14}$$

Equation (14) is the dynamics equation applied to a viscous non-compressible liquid imbibed in the cylindrical porous media. The liquid will reach a stationary level, h_∞, established by the balance of gravity and capillarity,

$$h_\infty = \frac{S_v\gamma_l \cos\theta}{\rho g\phi} \tag{15}$$

Structure parameters

In equation (14), S_v, τ, ϕ are the structure parameters of the porous media. d_h is related to the structure of the porous media. To determine the hydraulic diameter, the porous media is assumed to be a bundle of capillaries, and the total volume of which is the voids volume of the porous media, the total surface of which is the total surface area of the porous media. According to the definition of the hydraulic diameter, d_e is the ratio of the total voids volume to the surface area of the porous media. Then, the hydraulic diameter is given by

$$d_h = \frac{4V_{void}}{S_{surface}} = \frac{4V_{void}}{V_{total}} / \frac{S_{surface}}{V_{total}} = \frac{4\phi}{S_v} \tag{16}$$

In equation (16), V_{void} is the total voids volume, $S_{surface}$ is the total surface area, V_{total} is the total volume of the porous media.

From equations (14) and (15), we can see that the wicking phenomenon in porous media, is related to the structure parameters: S_v, τ, ϕ. Commonly, for porous media, the porosity, ϕ, is considered easy to obtain, and here the porosity ϕ is known. The specific surface S_v and the tortuosity τ can be calculated by numbers available models[29], which have a poor agreement with the natural porous media without empirical parameters.

The Boolean model is an important and versatile model for describing porous media. In this model, the pore centers are located obeying Poisson distribution in space V, as the result, the pores are allowed to overlap. And this model is related to the density of the pores and

the pore size distribution *f(r)*. For the Boolean model, the specific surface area is defined as[29]:

$$S_v = \nu[1-\phi]\overline{S} \tag{17}$$

In equation (17), ν is the pore number in unit volume porous media, and $\overline{S}=4\pi\int_{r_{\min}}^{r_{\max}} r^2 f(r)dr$, is the mean surface area of the pores.

Porous media have fractal features, and base on the fractal theory, the probability function for the pore distribution can be expressed as[30]:

$$f(r) = ar^{-1-D_f}, \qquad r_{\min} \le r \le r_{\max} \tag{18}$$

Where the factor a is found by normalizing the probability distribution function, D_f is the fractal dimension of the pores.

Therefore, the total volume of the pores in a unit cell can be calculated by:

$$\begin{aligned} V_p &= N_t \int_{r_{\min}}^{r_{\max}} \frac{4}{3}\pi r^3 f(r)dr = N_t a \int_{r_{\min}}^{r_{\max}} \frac{4}{3}\pi r^3 r^{-(D_f+1)}dr \\ &= \frac{4\pi}{3}\frac{r_{\max}^{3-D_f}}{3-D_f} N_t a[1-(\xi)^{3-D_f}] \end{aligned} \tag{19}$$

Where, N_t is the total pore number, $\xi = r_{\min}/r_{\max}$, and the volume of the unit cell can be obtained by:

$$V_u = \frac{V_p}{\phi} = \frac{4\pi}{3}\frac{N_t a}{\phi}\frac{r_{\max}^{3-D_f}}{3-D_f}[1-(\xi)^{3-D_f}] \tag{20}$$

The density of the pores ν is:

$$\nu = \frac{N_t}{V_u} = \frac{3}{4\pi}\frac{\phi}{a}\frac{3-D_f}{r_{\max}^{3-D_f}[1-(\xi)^{3-D_f}]} \tag{21}$$

As the definition, the mean surface area of the pores $\overline{S}$ is:

$$\begin{aligned} \overline{S} &= \int_{r_{\min}}^{r_{\max}} 4\pi r^2 f(r)dr = a\int_{r_{\min}}^{r_{\max}} 4\pi r^2 r^{-(D_f+1)}dr \\ &= \frac{4\pi r_{\max}^{2-D_f}}{2-D_f} a[1-(\xi)^{2-D_f}] \end{aligned} \tag{22}$$

Inserting equation (21) and (22) into equation (17), yields:

$$S_v = \frac{3\phi}{r_{\max}}\frac{3-D_f}{2-D_f}\frac{[1-(\xi)^{2-D_f}]}{[1-(\xi)^{3-D_f}]}(1-\phi) \tag{23}$$

The pore fractal dimension, D_f, can be calculated from[30]:

$$D_f = d - \frac{\ln\phi}{\ln\xi} \tag{24}$$

where d is the Euclidean dimension ($d = 3$ in this work). A correlation between the average tortuosity of flow path and porosity has been established experimentally by flow through beds packed with spherical particles[30]:

$$\tau = \frac{1}{2}\left[1+\frac{1}{2}\sqrt{1-\phi}+\sqrt{1-\phi}\,\frac{\sqrt{(\frac{1}{\sqrt{1-\phi}}-1)^2+\frac{1}{4}}}{1-\sqrt{1-\phi}}\right] \tag{25}$$

Cai et al. proposed a simple expression for calculating maximum pore diameter as[30]:

$$r_{\max} = \frac{D_s}{8}\left[\sqrt{\frac{2\phi}{1-\phi}}+\sqrt{\frac{\phi}{1-\phi}}+\sqrt{\frac{\pi}{4(1-\phi)}}-1\right] \tag{26}$$

Inserting equations (24), (25) and (16) into equation (14), an analytical capillary model for wicking in porous media can be obtained. In this model, the parameters D_s and ϕ can be obtained from experimental measurement whereas the quantities S_v, τ, $r_{\max}$ will be estimated using theoretical models. All the parameters have actual physical meaning, without empirical numbers.

DISCUSSION

It seems natural to take $h(0) = \dot{h}(0) = 0$ as the initial conditions to solve equation (14). However, because equation (14) has a singularity t = 0 when a finite force is applied to an infinitesimal mass, $m = Ah(t)\phi\rho(h \to 0)$, this would lead to an ill-posed problem. A way to solve this problem is to rewrite the first term on the right side of equation (14), in the form:

$$S_v\gamma_l\cos\theta = 32\tau^2\frac{h\mu\dot{h}}{\phi d_h^2}+\rho g\phi h+\rho\phi\left[(h+\lambda)\ddot{h}+\dot{h}^2\right] \tag{27}$$

where λ stands for some effective initial height[31]. It is necessary to introduce such a correction, as well as the meaning and order of magnitude of λ. For the constraint of flow continuity, the volume of liquid set into motion at the very beginning of capillary rise is not limited to the liquid which is absorbed in the porous media. At the same time, the liquid dipped part of the porous media and in the bulk, reservoir starts moving.

For the wicking phenomenon in a circular column porous media with sectional radius r_0, assuming the capillary just touches the liquid surface, as the result, the length of the dipped part is negligible compared to the anticipated lift. And the kinetic energy of the flow through a hemisphere of radius R centered in the entrance point must be equal to the flow through the capillary cross-section, thus:

$$\lambda\pi r_0^2\phi\dot{h}^2 = \int_{r_0}^{\infty} 2\pi r^2 v_{sphere}^2 dr \tag{28}$$

If Poiseuille flow is assumed:

$$v_{sphere} = \frac{1}{2}(\frac{r_0}{r})^2\dot{h} \tag{29}$$

Then,

$$\lambda = \frac{r_0}{2\phi} \tag{30}$$

which shows that the lower bound of the mass set into motion as the capillary rise commences is of the order of magnitude of $m = \pi r_0^3\rho/(2\phi)$. This simple argument shows that the capillary force always acts on a finite mass eliminates the initial burst. Therefore, the solution of equation (14) can be carried out numerically through the finite difference method.

Model comparison with experimental data

To verify the validity of the capillary model (equation 14), the accumulated imbibition weight in porous media is achieved by:

$$W = Ah(t)\phi\rho \tag{31}$$

where, W is the weight of the liquid imbibed in porous media, which is convenient to be got by experiment. $h(t)$ is the height of the liquid, obtained from equation (14). The theoretical predictions are tested using available experimental data from different literatures.

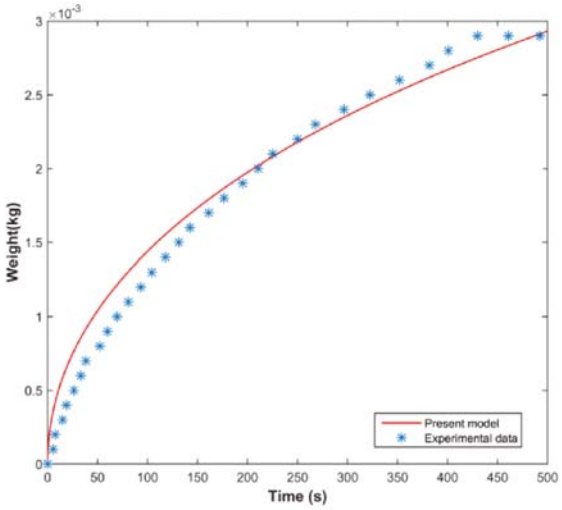

Figure 2. Comparison of the accumulated imbibition weight of water versus time by the present full analytical expression with experimental data in glass beads A[32]

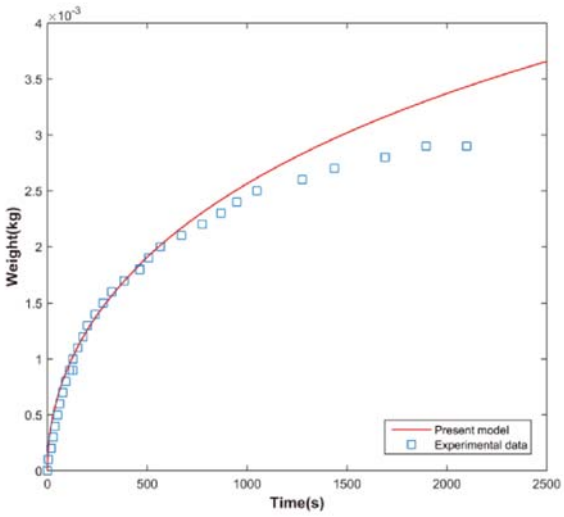

Figure 3. Comparison of the accumulated imbibition weight of water versus time by the present full analytical expression with experimental data in glass beads B[32]

In Figures 2 and 3, the imbibition weight calculated by the present full analytical expression was compared with the experimental data from Li et al. The measurement was made at 20°C, with water (γ=72.3mN/m, ρ=0.997g/cm^3, μ=1.01$mPa\cdot s$) imbibed in glass beads. The characteristics of glass beads are presented in Table 1. In Figures 2 and 3, the present model predictions have a good agreement with the experimental data. The contact angles $\theta = 65^o$ and $\theta = 68^o$, were used respectively, to fit the experimental data.

Table 1. Characteristics of bed of particles[32]

Symbol	Particle diameter, [μm]	Porosity	Bulk density,[kg/m^3]
A	185	0.366	1.31
B	255	0.371	1.30

However, the value of contact angles here is less than the value in the reference[32], which is 76°. This is because that the contact angles in reference[32] were obtained by the model without thinking about the effects of liquid inertia, which was considered in equation (14). As the result, the contact angles obtained here must be smaller, for the same imbibition weight of water. Figure 4 shows a comparison between the predictions of the present model and the experimental data obtained using Bentheim[33] sandstone cores. The porosity of the sandstone cores is 0.23, the cross-section is 5.15 cm^2. The characteristic particle diameter of D_s = 0.19 mm was used, to fit the experimental data.

From Figures 2, 3 and 4, we can see that the present model can fit the experimental data very well in the initial period of imbibition time. But after 1000 seconds in Figure 3, the experimental values of imbibition weight are lower than predictions from the present model. It is caused by the limited height of the porous media material[16]. When the imbibing water phase hits the top of the sample, the imbibition rate will drastically be slowed down causing the discrepancy between the model predictions and the experimental data.

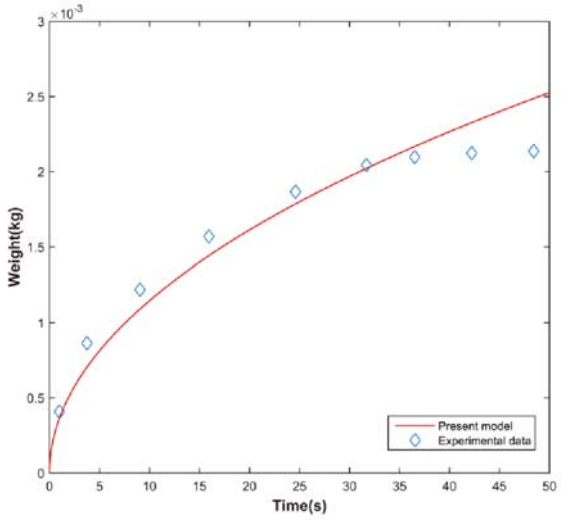

Figure 4. Comparison of the accumulated imbibition weight of water versus time by the present full analytical expression with experimental data in glass beads C[33]

Structure properties influence

Base on the analytical model, equation 14, the influence of the porous media structure properties on the imbibition process was discussed by considering water as the imbibing liquid displacing the air. Hence, the parameters γ=72.3mN/m, ρ=0.997g/cm^3, μ=1.01$mPa\cdot s$ were used in equation 14.

Figure 5 shows the imbibition height versus time at the different specific surfaces. From the picture, it is shown that the larger the specific surface, the longer time is needed to reach the equilibrium height. The numerical result agrees with equation 15. During the imbibing process, water in the porous media with lower specific surface, has higher rise rate, for the higher the viscous force.

In Figure 6, the imbibition height versus time at different porosity is described. As shown in the picture,

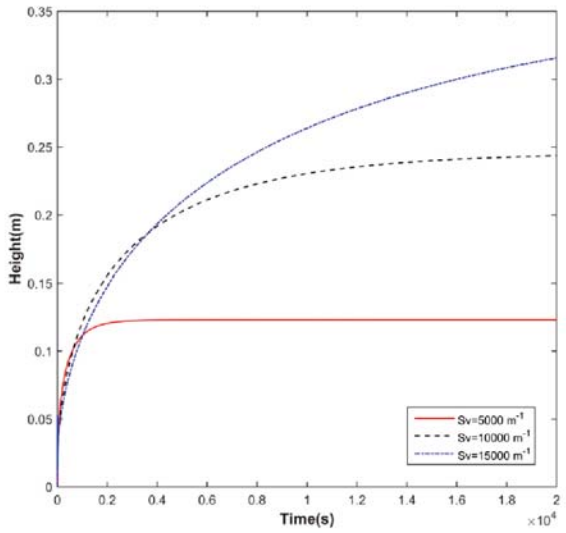

Figure 5. Plot of imbibition height versus time at different specific surface
(γ=72.3mN/m, ρ=0.997g/cm^3, μ=1.01$mPa\cdot s$, ϕ=0.3)

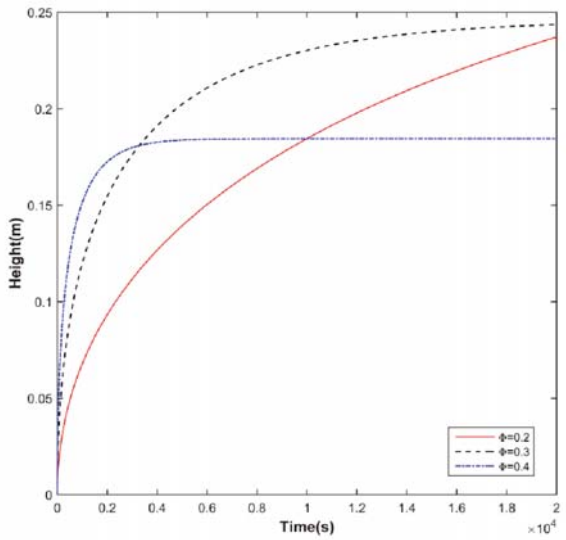

Figure 6. Plot of imbibition height versus time at different porosity
(γ=72.3mN/m, ρ=0.997g/cm^3, μ=1.01$mPa\cdot s$, Sv=10000m^{-1})

the lower the porosity is the longer time needed to reach the equilibrium height. Like the specific surface, the porosity influences the rising rate of the imbibition.

Figure 7 plots the imbibition height versus time at different tortuosity. Tortuosity does not influence the equilibrium height, from the picture. It is not difficult to find that the larger the tortuosity, the slower the water reaches the equilibrium height.

CONCLUSION

To sum up, a full theoretical model for the wicking behavior of wetting liquid into porous media based on statistical geometry was established in this paper. In the model, a new structure-property relationship was depicted in terms of a specific surface S_v, porosity θ, tortuosity τ, pore fractal dimension D_f, maximum pore size r_{max}, which have clear physical meaning. In addition, the accumulated imbibition weight in porous media was achieved to verify the theoretical model, and the

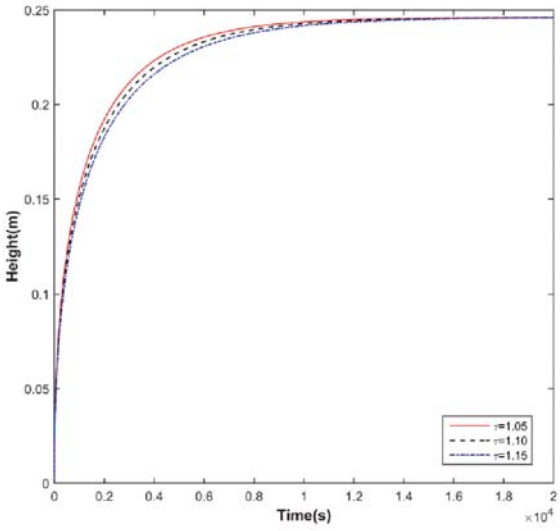

Figure 7. Plot of imbibition height versus time at different tortuosity
(γ=72.3mN/m, ρ=0.997g/cm^3, μ=1.01$mPa\cdot s$, ϕ=0.3, Sv=10000m^{-1})

predictions can fit the published experimental data very well. Base on the analytical model, the influence of the porous media structure properties on the imbibition process was discussed. The larger the specific surface and the tortuosity, the longer time is needed to reach the equilibrium height. On the contrary, the lower the porosity is the longer time needed to reach the equilibrium height. The model and results in this work are useful for the application of porous media in scientific research and industry.

LITERATURE CITED

1. Liu, M., Wu, J. & Gan, Y. (2018). Tuning capillary penetration in porous media: Combining geometrical and evaporation effects. *Int. J. Heat Mass Tran.* 123, 239–250. DOI: 10.1016/j.ijheatmasstransfer.2018.02.101.

2. Wang, Y., Li, Y. & Zheng, H. (2019). Equilibrium, kinetic and thermodynamic studies on methylene blue adsorption by Trichosanthes kirilowii Maxim shell activated carbon. *Pol. J. Chem. Technol.* 21(4), 89–97. DOI: 10.2478/pjct-2019-0044.

3. Yin, X., Ma, Y. & Wang, X. (2021). Increasing Effect of Water Clarifiers on the Treatment of Polymer-Containing Oil Production Sewage. *Pol. J. Chem. Technol.* 23(2), 20–26. DOI: 10.2478/PJCT-2021-0012.

4. Sönmez, S. & Arslan, S. (2021). Investigation of the effects on ink colour of lacquer coating applied to the printed substrate in the electrophotographic printing system. *Pol. J. Chem. Technol.* 23(2), 35–40. DOI: 10.2478/pjct-2021-0014.

5. Singh, K., Jung, M. & Brinkmann, M. (2019). Capillary-Dominated Fluid Displacement in Porous Media. *Annu. Rev. Fluid Mech.* 51, 429–449. DOI: 10.1146/annurev-fluid-010518-040342.

6. Washburn, W. (1921). The Dynamics of Capillary Flow. *Physical Review*, 17(3), 273–283.

7. Li, X., Xian, F. & Alexand, R. (2013). An experimental study on dynamic pore wettability. *Chem. Eng. Sci.* 104, 988–997. DOI: 10.1016/j.ces. 2013.10.026 .

8. Ramírez-Flores, J.C. & Bachmann, J. (2013) Analyzing capillary-rise method settings for contact-angle determination of granular media. *J. Plant. Nutr. Soil. Sci.* 176, 19–26. DOI: 10.1002/jpln.201100431.

9. Thakker, M., Karde, V. & Shah, D.O. (2013). Wettability measurement apparatus for porous material using the modified Washburn method. *Meas. Sci. Technol.* 24, 125902.

10. Thomas, E.A., Poritz, D.H. & Muirhead, D.L. (2013). Urine Advancing Contact Angle on Several Surfaces. *J. Adhes. Sci. Technol.* 23(19), 17–23. DOI: 10.1163/016942409X12508517390879.

11. Yang, B., Song, S. & Lopez-Valdivieso, A. (2014). Effect of Particle Size on the Contact Angle of Molybdenite Powders. *Mineral Processing & Extractive Metall. Rev.* 35, 208–215. DOI: 10.1080/08827508.2013.763802.

12. Tamayol, A. & Bahrami, M. (2011). Transverse permeability of fibrous porous media. *Phys. Rev E*. 83, 046314. DOI: 10.1103/PhysRevE.83.046314.

[13] Guo, P. (2012). Dependency of Tortuosity and Permeability of Porous Media on Directional Distribution of Pore Voids. *Transp. Porous Med*. 95(2012), 285–303. DOI: 10.1007/s11242-012-0043-8.

14. Li, K. (2010). More general capillary pressure and relative permeability models from fractal geometry. *J. Contam. Hydrol.* 111, 13–24. DOI: 10.1016/j.jconhyd.2009.10.005.

15. Cai, J. & Yu, B. (2011). A Discussion of the Effect of Tortuosity on the Capillary Imbibition in Porous Media. *Transp. Porous Med*. 89(2), 251–263. DOI: 10.1007/s11242-011-9767-0.

16. Cai, J., Hu, X., & Standnes, D.C. (2012). An analytical model for spontaneous imbibition in fractal porous media including gravity. *Colloids Surface A*. 414, 228–233. DOI: 10.1016/j.colsurfa.2012.08.047.

17. Dang, T. & Hupka, J. (2005). Characterization of porous materials by capillary rise method. *Physicochem. Probl. Mi.* 39(205), 47–65.

18. Stevens, N., Ralston, J. & Sedev, R. (2009). The uniform capillary model for packed beds and particle wettability. *J. Colloid Interf. Sci.* 337(1),162–169. DOI: 10.1016/j.jcis.2009.04.086.

19. Kramer, G.J. (1998). Static liquid hold-up and capillary rise in packed beds. *Chem. Eng. Sci.* 16(29), 85–92. DOI: 10.1016/S0009-2509(98)80001-8.

20. Chan, T.Y., Hsu, C.S. & Lin, S.T. (2004). Factors Affecting the Significance of Gravity on the Infiltration of a Liquid into a Porous Solid. *J. Porous Mat.* 11(4), 273–277. DOI: 10.1023/B:JOPO.0000046354.27879.9b.

21. Fries, N. & Dreyer, M. (2008). An analytic solution of capillary rise restrained by gravity. *J. Colloid Interf. Sci.* 320(1), 259–263. DOI: 10.1016/j.jcis.2008.01.009 .

22. Torquato, S. (2002). *Random Heterogeneous Materials: Microstructure and Macroscopic Properties*. NewYork, USA: Springer. DOI: 10.1115/1.1483342.

23. Elsner, A., Wagner, A. & Aste, T. (2009). Specific Surface Area and Volume Fraction of the Cherry-Pit Model with Packed Pits. *J. Phys. Chem. B*. 113(22), 7780–7784. DOI: 10.1021/jp806767m.

24. Hermann, H. (2010). Effective dielectric and elastic properties of nanoporous low-k media. *Modelling Simul. Mater. Sci. Eng*. 18(5), 055007. DOI: 10.1088/0965-0393/18/5/055007.

25. Li, K. & Zhao, H. (2012). Fractal Prediction Model of Spontaneous Imbibition Rate. *Transp. Porous. Med.* 91(2), 363–376. DOI: 10.1007/s11242-011-9848-0.

26. Masoodi, R., Languri, E. & Ostadhossein, A. (2013). Dynamics of liquid rise in a vertical capillary tube. *J. Colloid Interf. Sci.* 389(1), 268–272. DOI: 10.1016/j.jcis.2012.09.004.

27. John, C.B. (1993). *Wettability*. New York, USA: Elsevier.

28. Carman, P.C. (1937). Fluid flow through granular beds. *Trans. Inst. Chem. Eng*, 15, 32–48.

29. Hermann, H. & Elsner, A. (2014). Geometric Models for Isotropic Random Porous Media: A Review. *Adv. Mater. Sci. Eng.* (2014), 1–16. DOI: 10.1155/2014/562874.

30. Cai, J., Yu, B. & Zou, M. (2010). Fractal Characterization of Spontaneous Co-current Imbibition in Porous Media. *Energ. Fuel.* 24(2010), 1860–1867. DOI: 10.1021/ef901413p.

31. Zhmud, B.V., Tiberg, F. & Hallstensson, K. (2000). Dynamics of Capillary Rise. *J. Colloid Interf. Sci.* 228(2), 263–269. DOI: 10.1006/jcis.2000.6951.

32. Li, G. Chen, X. & Huang, Y. (2015). Contact Angle Determined by Spontaneous Imbibition in Porous Media: Experiment and Theory. *J. Disper. Sci. Technol.* 36(6), 772–777. DOI: 10.1080/01932691.2014.921627.

33. Olafuyi, O.A., Cinar, Y. & Knackstedt, M.A. (2007). Spontaneous imbibition in small cores. SPE Asia Pacific Oil and Gas Conference and Exhibition. 30 October 2007. Jakarta, Indonesia. DOI: 10.2118/109724-MS.